International Journal of Occupational Safety and Ergonomics (*JOSE*) 2011, Vol. 17, No. 3, 221–232

A Design of Experiments for Statistically Predicting Risk of Adverse Health Effects on Drivers Exposed to Vertical Vibrations

Houcine Ayari
Marc Thomas
Sylvie Doré

Department of Mechanical Engineering, École de technologie supérieure, Montréal, QC, Canada

An injury risk factor (IRF), which indicates the risk of adverse health effect to lumbar rachis arising from mechanical vibrations, is developed. Experiments have been conducted that consider acceleration levels at the seat of drivers, posture, morphology, density, damping rate and body mass as independent variables. A parametric finite-element model of the lumbar rachis has been generated. It is shown that the IRF increases with ageing and an IRF of 30% is proposed as a threshold for fatigue purposes. This level is reached if a peak acceleration level greater than 3 m/s^2 is applied to a light (55 kg) and an old driver with a low bone density and a damping rate of 20%. This vibration threshold must be reduced to 2.7 m/s^2 if the driver's weight increases to 75 kg and to 2 m/s^2 if the driver is heavy (98 kg).

adverse health effect whole-body vibration spinal loading finite-element analysis ageing design of experiments.

1. INTRODUCTION

Literature reports many epidemiologic investigations carried out to establish a link between exposure to upper body vibrations and low-back pain. This research shows a relationship between professional exposure to vertical vibrations transmitted to the upper body and an increased risk of adverse health effect. Long-term whole-body vibrations (WBV) can generate adverse health hazards for the lumbar spine, especially at the three lower vertebrae L3–L5 [1]. Several bibliographical reviews have indeed been published over the past 15 years; they show a higher occurrence of low back pain among populations exposed to dynamic loading, such as heavy-equipment drivers, than in the general population [2]. Available epidemiologic data are not, however, generally sufficiently powerful to establish a dose–effect relationship between exposure to WBV and the risk of lumbar disorders [3]. In fact, WBV induce dynamic stresses, principally compressive, into the spine, producing microfractures into the endplates and vertebral body. The long-term exposure of the human body to vibrations with the influence of different sitting postures, the effect of osseous density and the individual variability of the morphology, may lead to mechanical fatigue [4, 5] and low back pain due to microfractures in bones (cortical and cancellous) on endplates and microlesions in the intervertebral discs [6, 7, 8, 9]. Ayari, Thomas and Doré suggested that fatigue failure of vertebral endplates and cancellous bone could be the pathogenetic mechanism that caused subsequent degenerative changes of the lumbar spine [10]. Many researchers developed dynamic finite-element (FE) models of the human body [11, 12]. These studies provided useful information concerning the dynamic behaviour of the lumbar

The authors gratefully acknowledge the financial support provided by the Institut de Recherche en Santé et Sécurité du Travail (IRSST-Montréal) and the Natural Sciences and Engineering Research Council of Canada (NSERC) in providing grants.

Correspondence and requests for offprints should be sent to Marc Thomas, Department of Mechanical Engineering, École de technologie supérieure, 1100, Notre-Dame Street West, Montréal, QC, H3C 1K3, Canada. E-mail: <marc.thomas@etsmtl.ca>.

segments and were aimed at computing the forces acting on the spine for a specified acceleration level. However, few numerical studies established a relationship between the in vivo fatigue stresses and the acceleration at the seat. By applying an analytical method, Thomas, Lakis and Sassi studied the long-term adverse health effect for drivers exposed to harmonic and random vibrations [13]. Seidel, Blüthner, Hinz, et al.'s experimental study made it possible to assess a relationship between the forces and the acceleration at the seat by considering posture and the nature of the body (bone structure) [6]. However, most of these models used fixed parameters and were not designed to easily observe the effect of interindividual variations such as posture, bone structure, body weight, etc. In fact, a parametric FE model, such as the one developed by Lavaste, Skalli, Robin, et al. for a static analysis [14], is more suitable for an easy study of the various effects concerning anatomy or posture on dynamic behaviour. Consequently, this research is aimed at elucidating the relationship between exposure and vibratory response to derive quantitative relations for the assessment of the health risk in the vertebrae due to WBV by investigating the effect of the following parameters: driving posture, body weight, bone structure, apparent density (which is related to age), acceleration level and damping rate on dynamic stresses. These effects are taken into account to define safe limits of acceleration amplitudes measured at the seat.

2. SUBJECTS AND METHODS

2.1. Mathematical Model of the Injury Risk Factor

The dynamic behaviour of the vertebral bone may depend on several variables such as apparent density, age, gender, posture, loading, excitation frequency, modal parameters and several other factors. In this study, we considered the following parameters important: posture angle θ (°), body mass M (kg), cross-sectional area at the intervertebral disc S to represent the bone structure (m^2), apparent density ρ of lumbar vertebrae (kg/m^3), acceleration amplitude applied to the seat A (m/s^2), frequency of excitation f (Hz), natural frequency f_n (Hz) and damping rate ξ. If we consider a single-degree-of-freedom model as suggested by Griffin [15] for modelling the human body exposed to mechanical vibrations, the force transmitted to the lumbar spine can be evaluated. The force transmitted to the body F_T (N) may be expressed as

$$F_T = \frac{\sqrt{1+\left(2\xi\frac{f}{f_n}\right)^2}}{\sqrt{\left(1-\left(\frac{f}{f_n}\right)^2\right)^2+\left(2\xi\frac{f}{f_n}\right)^2}} M(2\pi f)^2 Y, \quad (1)$$

where F_T—transmitted force, ξ—damping rate, f—frequency of excitation, f_n—natural frequency, Y—excitation displacement from the seat.

By assuming that the excitation produces a vibration at the natural frequency ($f = f_n$) because the drivers are usually exposed to random or transient excitations, a simplified model for computing the dynamic stresses σ_{dyn} (Pa) has been developed from the transmitted force formulation by considering the morphology of the body (M, S and θ):

$$\sigma_{dyn} = P\frac{\sqrt{1+(2\xi)^2}}{2\xi}\frac{A \bullet M}{S}\cos(\theta), \quad (2)$$

where σ_{dyn}—dynamic stress, P—statistical constant, ξ—damping rate, A—acceleration amplitude applied to the seat, M—body mass, S—cross-sectional area at the intervertebral disc, θ—the posture angle;

By assuming that the risk of adverse health is relative to the ratio of the applied stress to the ultimate stress σ_u, an injury risk factor (IRF) was [16]

$$IRF = 100 \bullet \frac{(\sigma_{dyn} + \sigma_{stat})}{\sigma_u}, \quad (3)$$

where σ_{dyn}—dynamic stress, σ_{stat}—compressive static stress as computed with our numerical model.

The ultimate stress of the vertebrae σ_u, has been estimated from literature at $41.668\,\rho^{1.9}$ [9, 17]. σ_u for the whole vertebrae was assumed the same as that of the cancellous bone because

most fractures appear in this type of bone. By introducing Equation 2 into Equation 3, the following relationship has been developed:

$$IRF = \left(B_1 + B_2 \bullet \frac{\sqrt{1 + (2\xi)^2}}{2\xi} A \bullet M \cos(\theta) \right) \frac{1}{S \bullet \rho^{1.9}}, \quad (4)$$

where B_1, B_2—statistical constants, ξ—damping rate, A—acceleration amplitude applied to the seat, M—body mass, S—cross-sectional area at the intervertebral disc, ρ—apparent density.

2.2. FE Model

A parametric FE model of the rachis (L1/L5) was developed for studying the effects of postures (flexed, lordosis and neutral), bone structure (frail, medium and robust), body weight, degree of degeneration due to ageing as represented by the damping rate and apparent density on the IRF computed for different levels of acceleration. The parametric FE model of the lumbar spine (L1–L5) was generated by considering the parametric equations describing the shape of vertebra and intervertebral disc, as established by Lavaste et al. [14]. The morphometric dimensions were considered as measured on various vertebral bodies by Berry, Moran, Berg, et al. [18]. The main advantage of using a parametric model was the facility with which different human morphologies could be studied (any condition of posture as well as the effect of interindividual geometrical variations). The details of the FE model can be found in Ayari, Thomas, Doré et al. [19]. Nine geometrical models of the spine were generated for numerically extracting data which would be used for the design of experiments: three postures (flexed, lordosis and neutral) and three bone structure (frail, medium and robust). Figure 1 shows the FE model of the lumbar spine. The aspect of bone remodelling, while very

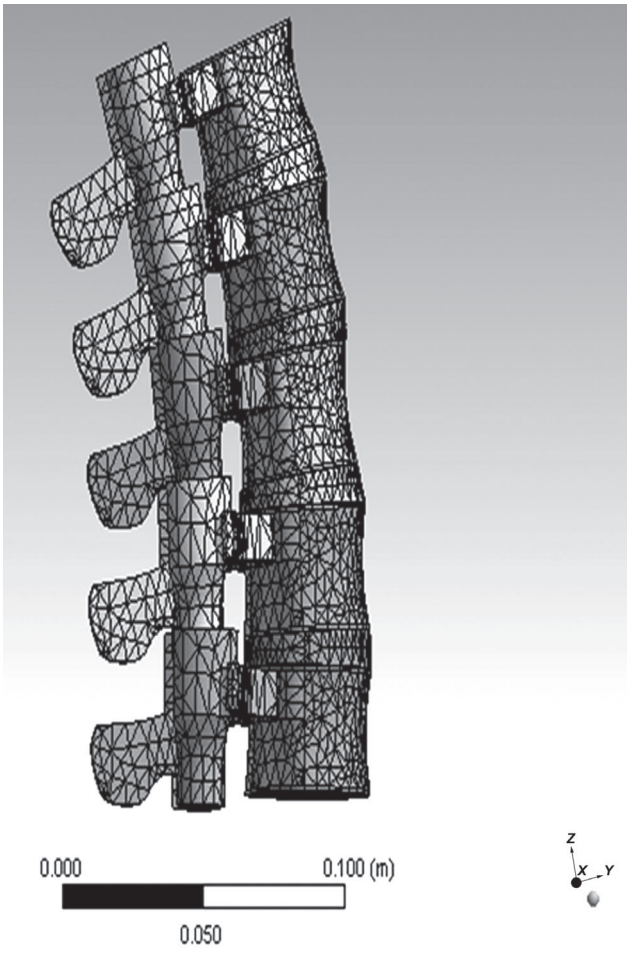

Figure 1. Finite-element model of lumbar spine.

important in fatigue concept, was not considered in this study which was aimed at developing a criterion based on an instantaneous IRF. The IRF contains the information on ultimate stress and consequently on ageing by varying density and damping.

Once the lumbar spine model was generated, the dynamic analyses were carried out on the model to compute the dynamic stresses. For the dynamic analysis of the lumbar spine, a distributed mass of ~55% of the total body mass was applied to the upper face of the rachis [20] to model the upper body. The mechanical properties of the various elements (cortical shell, cancellous bone, posterior elements and cartilaginous endplates, intervertebral disc) forming the vertebral body were taken from literature [21].

2.3. Range of IRF

Data from Standard No. ISO 2631-5:2004 [22] and from Brinckmann, Biggemann and Hilweg [7] were used to established IRF thresholds. In this study, the IRF is defined as the ratio between the calculated stress (or the stress recommended by Standard No. ISO 2631-5:2004) and the ultimate stress. The apparent density ρ may be described as a relationship with the number of years of exposure of drivers, e.g., for an old driver (65 years old) ρ = ~0.18 g/cm^3. Considering the ISO 2631-5:2004 limits, it appears that the equivalent IRF threshold for a 65-year-old driver is 30–50%. Furthermore, Brinckmann et al. argued that a stress ratio of 30% normalised with the ultimate stress could be estimated as an endurance limit for in vivo exposure [7]. The threshold of 30% may thus be assumed as a limit for avoiding any risk of fatigue after long exposure to dynamic excitations as it is usual in mechanical fatigue problems and, consequently, *IRF* = 30% could be considered as representing a moderate probability of injury. This threshold is also in agreement with the recommended stresses for an older driver, by considering a stress level σ = 0.5 MPa as a moderate probability of injury [22]. Furthermore, Hansson, Keller and Johnson's results showed that σ > 50% of the ultimate stress σ_u, induced fatigue failure occurring before 1000 cycles [9]. This threshold is in agreement with the recommended stresses for an older driver by considering σ = 0.8 MPa as a high probability of injury [22]. Consequently, we considered the following criteria for the IRF:

- if IRF < 30%, a driver working 240 days a year will have a low probability of injury;
- If 30% < IRF < 50%, a driver working 240 days a year will have a moderate probability of injury;
- If IRF > 50%, a driver working 240 days a year will have a high probability of injury.

2.4. Protocol of the Design of Experiments

To study the effects of parameters in Equation 4 on the IRF, a numerical design of experiments was conducted. A full factorial design was selected to allow all three-level interactions between the independent variables to be effectively investigated. The levels for each factor were extracted from literature.

- The lower face of vertebrae was subjected to various vertical *A*. The values of *A* were extracted from Standard No. ISO 2631-1:1997 [23] guides that define limits of exposure according to the frequency and duration of exposure. In this study, four levels were considered; *A* = 1, 2, 3.15, 4 m/s^2.
- The cancellous bone, representing almost 90% of the total volume of the vertebrae is porous and its fundamental role is to absorb energy. The elastic and strength properties of cancellous bone display substantial heterogeneity with respect to age, health, anatomical site, loading direction and loading mode. Both modulus and strength depend heavily on apparent density. In compression, both modulus and strength decrease with age, by ~10% per decade [24]. These relationships vary for different types of cancellous bone because of the anatomic site, age and disease and related variations in cancellous architecture. Linear and power-law relationships can be used to describe the dependence of modulus and compressive strength on apparent density and age [25], with

typical coefficients of determination R^2 = .6–.9. ρ of the cancellous bone of the vertebrae (g/cm^3) decreases linearly with age [26]. ρ may be described as a linear relationship with the number of years n of exposure of drivers [24]:

$$\rho = 0.375 - 0.003\ (n + 25), \qquad (5)$$

where ρ—apparent density, n—number of years of exposure from 25 years. For a young 25-year-old driver (n = 0), ρ = 0.3 g/cm^3; ρ = 0.1, 0.2, 0.3 g/cm^3 was considered.

- In seated posture, three critical levels of θ were chosen as determined by Adams, Bogduk, Burton, et al. [27]: flexed ($\theta \leq 5^\circ$), lordosis ($\theta \geq 25^\circ$) and neutral ($\theta \approx 15^\circ$).
- Three levels of S were considered; S at L3–L4 represents the bone structure (frail, medium or robust body). Seidel et al. used the same parameter [6]. In fact, Seidel et al. considered two main parameters to define the bone structure, S and the humeral index represented by the ratio between elbow width and the length of the upper arm.
- The viscous ξ depends on the degree of degeneration of the intervertebral disc (grade of the disc) and muscle activity [27]. We may consider ξ = 30% for a young 25-year-old driver. For a driver older than 25 years, the following a linear relationship with the number of years of exposure may be assumed:

$$\xi = 0.3 - 0.0025\ n, \qquad (6)$$

where ξ—damping rate, n—number of years of exposure from 25 years. The stress responses were computed by considering viscous ξ = 10, 20, 30% as determined by Kasra, Shirazi-Adl and Drouin [21] and Izambert, Mitton, Thourot, et al. [20].
- Three levels of body weight were chosen (light, medium, heavy).

Table 1 summarizes the values considered for each factor. There were 972 numerical simulations.

3. RESULTS

3.1. Analysis of Variance

The main effects of independent variables, together with their three-level interaction effects on the IRF, were calculated with analysis of variance (ANOVA). The ANOVA demonstrates the variability of the IRF through its contributing factors. P and the Fisher ratio (F ratio) test the significance of each factor and the interaction between them. The higher the F ratio and the closer the P value to zero, the more significant the effect. For the ANOVA analysis, we selected a 99% confidence level ($P < .01$) for testing the significance of the main effects and three-level interaction effects. Table 2 shows the computed ANOVA output and the calculated F ratio with their P values for each significant effect. The effects are classified from the most to the least significant one.

TABLE 1. Independent Variables for the Design of Experiments

	Level			
Variables	**1**	**2**	**3**	**4**
Acceleration A (m/s^2)	1	2	3.15	4
Apparent density ρ (g/cm^3)	0.1	0.2	0.3	—
Body mass M (kg)	55	75	98	—
Posture angle θ (°)	5	15	25	—
Cross sectional area L3–4 S (mm^2)	1200	1500	1800	—
Damping rate ξ (%)	10	20	30	—

TABLE 2. ANOVA Results (P = 0.0)

Source	*SS*	*df*	*MS*	*F* Ratio
	Main effects			
Apparent density ρ	1.42295E6	2	711473	76191
Body weight *M*	143422	2	71711	7679
Damping rate ξ	97634	2	48817	5228
Acceleration *A*	91415	3	30471	3263
Cross-sectional area *S*	51768	2	25884	2772
Posture angle θ	5493	2	2746	294
	Three-level interactions			
$M \times \rho \times \xi$	10185	8	1273	136
$A \times \rho \times \xi$	14604	12	1217	130
$A \times M \times \rho$	5519	12	460	49
$M \times S \times \rho$	3533	8	442	47
$M \times S \times \xi$	2212	8	276	30
$A \times M \times \xi$	2894	12	241	26
$S \times \rho \times \xi$	1491	8	186	20
$A \times S \times \rho$	1600	12	1335	14
$M \times \theta \times \rho$	670	8	84	9
$\theta \times \xi \times \rho$	636	8	80	9
Residual	6424	688	9	—
total (corrected)	2.18576E6	971		

Notes. All *F* ratios are based on the residual mean square error.

3.2. Effects on the IRF

In the following analysis, we considered 30 and 50% as thresholds of IRF. Sections 3.2.1.–3.2.4. examine the four main combinations of three-level interactions.

3.2.1. Interactions between ρ and ξ and M

Figure 2 shows the interactions between the body mass *M*, damping ξ and density ρ. The IRF increases with *M* and when ρ and ξ decrease. Statistical results show that young drivers with high bone density (ρ = 0.3 g/cm^3) present low risks whatever *M* and ξ. On the other hand, the IRF is very critical when ρ is very low (ρ = 0.1 g/cm^3), whatever *M* and ξ. Workers with high ξ (ξ = 30%) present low risk if ρ > 0.1 g/cm^3. In fact, medium ρ of 0.2 g/cm^3 represents a threshold for a risk of damage, depending on drivers' *M* and ξ. The

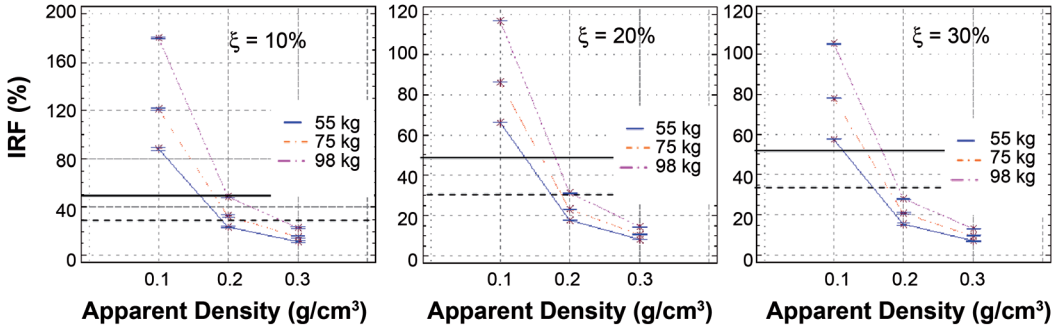

Figure 2. Interactions between mass, density and damping (ξ). *Notes.* IRF—injury risk factor.

effect of *M* is critical especially for low damping ($\xi = 10\%$) and medium ρ.

3.2.2. Interactions between A, ξ *and* ρ

The damping ξ, the density ρ and the acceleration *A* are the second most important significant three-level interaction (Figure 3). As expected, the risk increases with *A*. Figure 3 shows that *A* must be controlled to $A < 4$ m/s^2 to avoid a high probability of injury to drivers having low ξ ($\xi = 10\%$) and $\rho = 0.2$ g/cm^3. However, by considering the endurance limit of 30%, *A* must be <2 m/s^2 to avoid a moderate probability of injury. It is also shown that the IRF decreases with increasing ρ and ξ. The negative effect on the IRF is critical when density is very low ($\rho <$ 0.2 g/cm^3). Indeed, ρ is nonlinear since the IRF varies more between 0.2 and 0.1 g/cm^3 than between 0.3 and 0.2 g/cm^3 whatever ξ. Drivers with $\xi > 10\%$ and $\rho > 0.2$ g/cm^3 present low risks whatever *A* while vertebrae with low ξ of 10% combined with $\rho = 0.2$ g/cm^3 present a moderate risk when exposed to vibration amplitudes greater than 2 m/s^2. Consequently, $\rho = 0.2$ g/cm^3 may be considered as a threshold for the risk of damage, depending on *A* and ξ.

3.2.3. Interactions between A, *M and* ρ

The third most important effect is the interaction between the acceleration *A*, the body mass *M* and the density ρ (Figure 4). As seen previously, the IRF is low for a driver with high density ($\rho = 0.3$ g/cm^3) while the IRF becomes very high with ageing and loss of density ($\rho = 0.1$ g/cm^3), whatever *M* or the vibration level. With $\rho = 0.2$ g/cm^3, the amplitude of vibration must be controlled to less than 4 m/s^2 to avoid a risk of injury for drivers with $M < 75$ kg and to less than 2 m/s^2 to permit long-term exposure for heavy drivers ($M = 98$ kg).

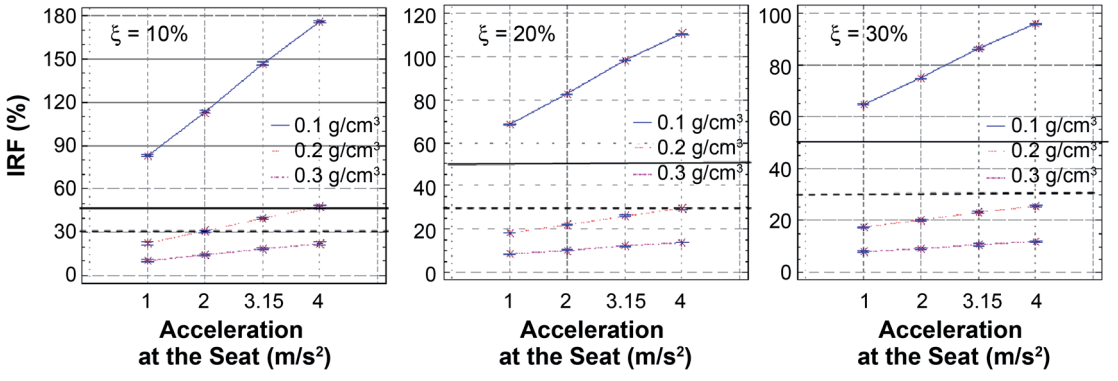

Figure 3. Interactions between acceleration, damping (ξ) and density. *Notes.* IRF—injury risk factor.

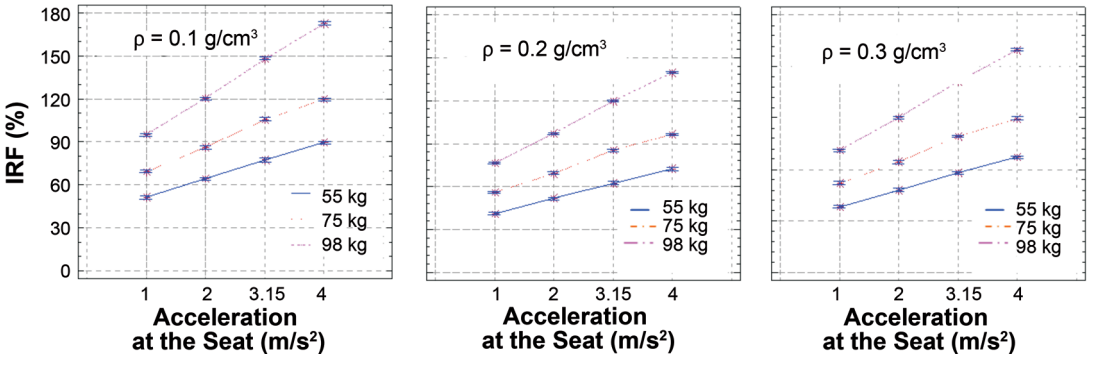

Figure 4. Interactions between acceleration, mass and density (ρ). *Notes.* IRF—injury risk factor.

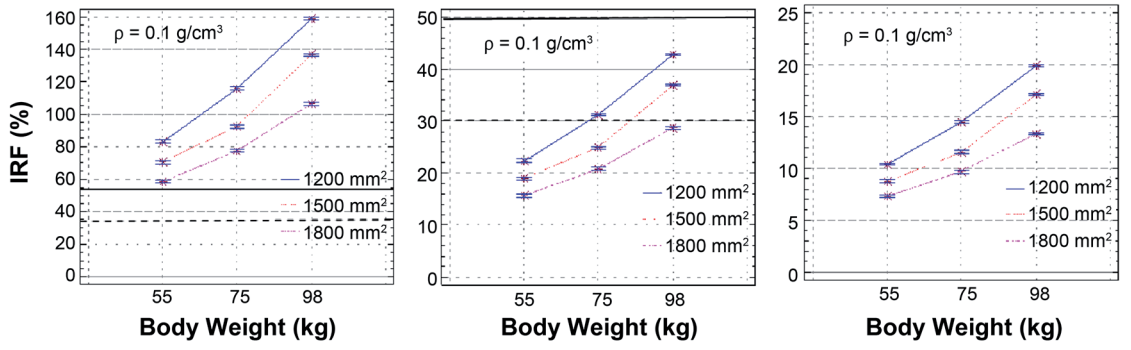

Figure 5. Interaction between mass, cross-sectional area at the disc and density (ρ). *Notes.* IRF—injury risk factor.

3.2.4. Interactions between M, S *and* ρ

Figure 5 shows the effects of the body mass *M*, the cross-sectional area at the intervertebral disc *S* and the density ρ on IRF. IRF increases with *M* and with a decrease in *S* and ρ. The IRF is very high if the density is low (ρ = 0.1 g/cm^3), while there is a low probability of injury when density is high (ρ = 0.3 g/cm^3). When ρ = 0.2 g/cm^3, heavy drivers (*M* = 98 kg) present a risk if *S* < 1800 mm^2.

3.2.5. Synthesis

In compression, both modulus and strength of bone decrease with ageing, falling ~10% per decade [24]. Both modulus and strength depend heavily on the apparent density ρ. Thus, the IRF can be expressed depending on *A*, ρ and ξ, which take into account the aging process, *M* and *S*, which represent the morphology. The parametric model has been applied for computing the stresses and the IRF when *A* = 1, 3, 6 m/s^2 are applied to three types of drivers with different ages (ρ and ξ) and morphologies (*M* and *S*):

- a young driver of 25 years with ρ = 0.3 g/cm^3 and ξ = 30%;
- a driver of 45 years with ρ = 0.24 g/cm^3 and ξ = 25%; and finally
- an older driver of 65 years with ρ = 0.18 g/cm^3 and ξ = 20%.

The results are shown in Table 3.

The stresses and the IRF computed with finite elements show that a healthy young driver presents few risks of injury. At 25 and 45 years old, the IRF of drivers is low (IRF ≤

TABLE 3 Risk of Injury According to Morphology and Ageing

			Effect of Morphology								
Effect of Morphology and Ageing			Light Weight			Medium Weight			Heavy Weight		
Effect of ageing	25 years old	*A* (m/s^2)	1	3	6	1	3	6	1	3	6
	ρ = 0.3 g/cm^3	IRF (%)	7	10	14	8	11	15	9	12	16
	ξ = 30%	σ_{tot} (MPa)	0.31	0.42	0.58	0.34	0.46	0.63	0.37	0.5	0.7
	45 years old	*A* (m/s^2)	1	3	6	1	3	6	1	3	6
	ρ = 0.24 g/cm^3	IRF (%)	12	16	23	13	17.5	25	14	19	27
	ξ = 25%	σ_{tot} (MPa)	0.32	0.44	0.62	0.35	0.48	0.70	0.38	0.53	0.75
	65 years old	*A* (m/s^2)	1	3	6	1	3	6	1	3	6
	ρ = 0.18 g/cm^3	IRF (%)	21	30	44	23	33	48	25	36	52
	ξ = 20%	σ_{tot} (MPa)	0.33	0.48	0.7	0.36	0.53	0.77	0.4	0.57	0.84

Notes. ρ—apparent density, ξ—damping rate, *A*—applied acceleration at the seat, IRF—injury risk factor, σ_{tot}—total compressive stress (dynamic stress σ_{dyn} + compressive static stress σ_{stat}). Grey highlights high levels of the IRF.

30%), whatever *M* even if exposed to as high as $A = 6$ m/s^2. However, the IRF becomes moderate to high for drivers 65 years old with low ρ and ξ. In fact, *A* must be controlled to $A < 6$ m/s^2 for drivers with $\xi = 20\%$ and $\rho = 0.18$ g/cm^3. Furthermore, *A* must be reduced to $A = 3$ m/s^2 for drivers with low *M*, to $A = 2.7$ m/s^2 for medium *M* and to $A = 2$ m/s^2 for high *M*. $A = \sim 3$ m/s^2 can produce a total compressive stress ($\sigma_{tot} = \sigma_{dyn} + \sigma_{stat}$) of 0.5–0.8 MPa and for this *A*, IRF < 36%, whatever the age of drivers and *M*.

3.3. Modelling the IRF

The next step is to develop the best possible prediction model for IRF using the full set of data. By performing a nonlinear regression analysis on parameters, a model describing the relationship between IRF and the independent variables has been obtained. The equation of the fitted model becomes

$$IRF = \frac{1}{S \bullet \rho^{1.9}} \left(715.106 + 1.75 \frac{\sqrt{1+(2\xi)^2}}{2\xi} A \bullet M \bullet \cos(\theta) \right), \text{ with } R^2 = .957, \quad (7)$$

where *S*—cross-sectional area at the inter-vertebral disc, ρ—apparent density, ξ—damping rate, *A*—acceleration amplitude applied to the seat, *M*—body mass, θ—posture angle.

The adjusted R^2 statistic (correlation co-efficient), which is more suitable for comparing models with different numbers of independent variables, indicates that this model explains 95% of the variability in IRF.

4. DISCUSSION

To validate the model of prediction of the IRF, the numerical results of the computed forces have been compared with those published in literature. The compressive forces have been computed at the level of the motion segment L3–L4 for an average person ($\theta = 15°$, $S = 1500$ mm^2, $M = 75$ kg, $\xi = 10, 20, 30\%$). This segment and those parameters were chosen to compare our results with those in the literature. These forces can be estimated for various acceleration amplitudes applied to the seat. For a medium area and $M = 75$ kg, the dynamic maximum compressive force transmitted at L3–L4 by applying $A = 3.15$ m/s^2 at the vertical resonant frequency, is computed at 721, 380 and 275 N for ξ of 10, 20 and 30% respectively. The maximal compressive force, combining static and dynamic efforts, acting at L3–L4 segment is 675–1121 N, depending on ξ. The dynamic stresses σ_{dyn} were determined from our dynamic model. In the literature, few articles on the dynamic forces applied to the lumbar spine were found. Through experiments, Fritz determined a maximum load at level L3–L4 of 634 N for $A = \sim 4.9$ m/s^2 [12]. Verver, van Hoof, Oomens, et al. estimated the compressive and tangential loads on the whole spine (from interface L5–S1 to interface C1–C2) [11]. At resonance, the compressive load on level L3–L4, for $A = 3.9$ m/s^2, ranged from 581 to 852 N according to the type of seat. Hinz, Blüthner, Menzel, et al. developed a biomechanical model for the determination of the compressive load at level L3–L4 by using an effective weight of the human body on L3–L4 and relative $A = 2.9$ m/s^2 [28]. The maximum load was estimated at 657 N. Thomas et al. showed that a healthy driver working 240 days a year could have a high probability of an adverse health effect after 12 years of continuous work if he was exposed to an harmonic excitation with $A > 3.15$ m/s^2, which produces a compressive force ~980 N [13]. Table 4 shows that the forces, computed in the present study, are in the same range than those reported in literature, with some higher values. The overestimation (1120 N) can be explained by the fact that the excitation was applied at the natural frequency of the system.

There is a nonlinear relationship between σ_{dyn} at the resonant frequency, ξ, θ, *M*, *S* and *A*. The model of prediction of σ_{dyn} has been compared to Seidel et al.'s results [6]. They developed from experiments a model to estimate the mean dynamic and the total stresses at L5/S1 for young people (21 years old) with mean $M = 68$ kg, $S = 1753, 1963, 2024$ mm^2, and two posture

TABLE 4. The L3–L4 Maximum Compressive Forces Compared to Those Published in Literature

Dynamic Forces From Literature	Frequency Range (Hz)	Maximal Acceleration at the Seat (m/s^2)	Maximum Compressive Forces (N)
Present study	0.5–15.0	3.1	675–1120
Thomas, Lakis & Sassi [13]	4–8	3.1	980
Verver, van Hoof, Oomens, et al. [11]	0.5–15.0	4	581–852
Fritz [12]	0–30	1–5	634
Hinz, Blüthner, Menzel, et al. [28]	0.5–7.0	3.1	657

angles: the driving posture *D* and the bend forward posture *BF*. The total compressive stress ($\sigma_{tot} = \sigma_{dyn} + \sigma_{stat}$) was related to *S*, θ and *A*. The damping was not considered (ξ = ~30% for a young driver). Figure 6 illustrates the relationship between σ_{tot} and *A* computed at the natural frequency of the lumbar spine in vertical direction by our numerical model and Seidel et al.'s model. The results show that the stresses that are obtained from our numerical model agree very well with Seidel et al.'s model, for a similar anatomy. However, our new model presents the advantage of considering the effect of damping that refines the results determined by Seidel et al.

The IRF (Equation 7) may also be expressed according to *A*, age and corresponding ρ and ξ. For a medium body of different ages (medium area $S = 1500$ mm^2), medium body mass ($M = 75$ kg) and a neutral posture angle ($\theta = 15°$), Figure 7 shows the relationship between the IRF and *A* when the excitation frequency is equal to the natural frequency ($f = f_n$, as when exposed to random or transient vibrations).

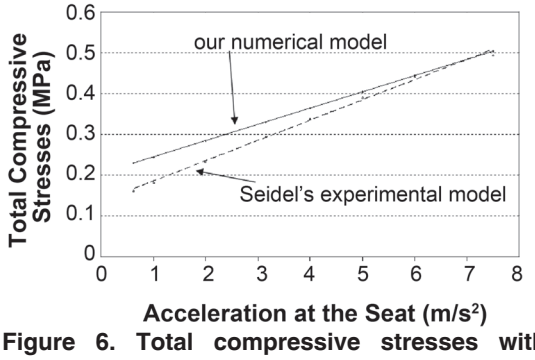

Figure 6. Total compressive stresses with accelerations at the seat, at resonant frequency for a damping rate of 30% (cross-sectional area at the disc $S = 1963$ mm^2, body mass $M = 69$ kg).

As expected, the results show that the IRF increases with age because ρ and ξ decrease.

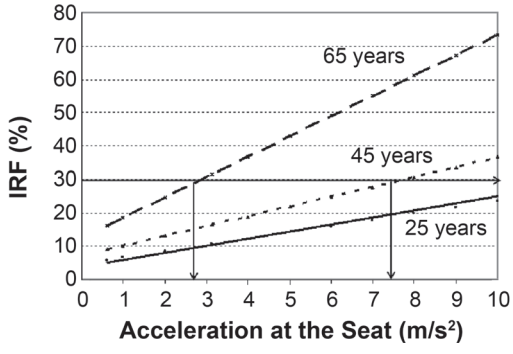

Figure 7. Injury risk factor with acceleration amplitude at the seat.

When considering a healthy person, $A = 3$ m/s^2 was applied at the seat at the spine natural frequency can produce an IRF of only 11% for a young driver (25 years old) by considering $\rho = 0.3$ g/cm^3 and ξ = ~30%, while for the same level of excitation the IRF increases to 17.5% for a 45-year-old driver ($\rho = 0.24$ g/cm^3, ξ = 25%) and to 33% when the driver is 65 years old ($\rho = 0.18$ g/cm^3 and ξ = 20%). In fact, *A* recorded at the seat has no significant effect for young drivers (25 years old). However, it must be limited to amplitudes under 7.5 m/s^2 for a 45-year-old driver and under 2.7 m/s^2 for a 65-year-old driver, if the excitation is maintained at the natural frequency of the lumbar spine, as in the case when driving on roads that produce shocks or random excitations. This level must be reduced $A = 2$ m/s^2 if $M = 98$ kg. The prescribed levels can be compared to the 2-m/s^2 limit for a very uncomfortable level as defined by Standard No. ISO 2631-1:1997 [23].

Equation 8 shows the relationship between the acceleration threshold ($A_{30\%}$) at the site and the age of drivers for a medium body ($S = 1500$ mm^2, $\theta = 15°$ and $M = 75$ kg):

$$A_{30\%} = -0.232\,Year + 17.863, \qquad (8)$$

where $A_{30\%}$—the acceleration threshold at the seat (m/s^2), *Year*—driver' age (in years).

5. CONCLUSION

The method of designing experiments makes it possible to statistically analyse results that show a large variability between individuals, such as weight, size, gender, age, etc. An FE model of lumbar spine was developed by using a parametric model because this strategy allows a very quick simulation of various anatomies (robust, average or frail body-types). The dynamic model that has been developed is aimed at computing the dynamic mechanical stresses of the lumbar spine produced by WBV of a person in a seated position to evaluate the risk of adverse health effects, which could occur for professional drivers by considering the effect of θ, ξ, *M*, *S* and ρ. This parametric FE model was validated by using published results of forces calculated at L3–L4 and the experimental dynamic stresses estimated at L5–S1. An IRF was developed for any given vibratory amplitude coming from the seat. From 972 computations, an ANOVA analysis revealed that ρ was definitely the most important factor affecting the IRF. The effects of the interactions combining ρ and ξ were found more significant than all the other combinations of variables on the IRF. It was found that the risk of adverse health was more significant if $\rho < 0.2$ g/cm^3 and if $\xi < 20\%$.

These effects are related to the age of drivers and this study confirms that older drivers have a more significant probability of injury than younger ones. If IRF = ~30% is defined as a limit of endurance to avoid fatigue problems, the results show that drivers older than 45 years old are susceptible to long-term injury and that their *M* has a significant effect. If we consider a driver with a low *M* and $\rho = 0.2$ g/cm^3, an excitation $A = 3$ m/s^2 applied to the seat has been considered as a threshold limit to have a small probability of injury. This vibration threshold must be reduced to 2.7 m/s^2 if *M* increases to 75 kg and to 2 m/s^2 if $M = 98$ kg. Consequently, $A < 2$ m/s^2 (1.4 m/s^2 rms) if we want to avoid any risk of injury whatever the driver, weight, bone structure and age.

REFERENCES

1. Bovenzi M, Hulshof C. An updated review of epidemiologic studies on the relationship between exposure to whole-body vibration and low back pain (1986–1997). Int Arch Occup Environ Health. 1999;72(6):351–65.
2. Lings S, Leboeuf-Yde C. Whole-body vibration and low back pain: a systematic, critical review of the epidemiological literature 1992–1999. Int Arch Occup Environ Health. 2000;73(5):290–7.
3. Pope MH, Wilder DG, Magnusson M. Possible mechanics of low back pain due to whole-body vibration. J Sound Vib. 1998;215(4):687–97 DOI:http://dx.doi.org/10.1006/jsvi.1998.1698).
4. Thomas M. A theoretical model for predicting fatigue limits of lumbar spine incurred to random vibration exposure during driving, In: Shayan E, editor. The 26th International Conference on Computers & Industrial Engineering. Hawthorn, VIC, Australia: Swinburne University of Technology; 1999. p. 419–23
5. Sandover J. The fatigue approach to vibration and health: is it a practical and viable way of predicting the effects on people? J Sound Vib. 1998;215(4):699–721 (DOI:http://dx.doi.org/10.1006/jsvi.1998.1605).
6. Seidel H, Blüthner R, Hinz B, Schust B. On the health risk of the lumbar spine due to whole-body vibration—theoretical approach, experimental data and evaluation of whole-body vibration. J Sound Vib. 1998;215(4):723–41 (DOI:http://dx.doi.org/10.1006/jsvi.1998.1601).
7. Brinckmann P, Johannleweling N, Hilweg D, Biggemann M. Fatigue fracture of human lumbar vertebrae. Clin Biomech (Bristol, Avon). 1987;2(2);94–6.
8. Pope MH, Hansson TH. Vibration of the spine and low Back pain. Clin Orthop Relat Res. 1992;279:49–59.
9. Hansson TM, Keller T, Johnson R. Mechanical behaviour of the human lumbar

spine. II. Fatigue strength during dynamic compressive loading, J Orthop Res. 1987:5(4):479–87.

10. Ayari H, Thomas M, Doré S. Développement d'un modèle statistique de prédiction de la durée de vie du rachis lombaire, dépendant de la contrainte appliquée, de l'âge et de la densité osseuse [Statistical model development for predicting life time of lumbar rachis, according to cyclic stresses, age and bone density]. Perspectives Interdisciplinaires Sur le Travail Et la Santé (PISTES). 2005:7(2):1–14. Retrieved July 26, 2011, from: http://www.pistes.uqam.ca/v7n2/articles/v7n2a8.htm
11. Verver MM, van Hoof J, Oomens CW, Van De van de Wouw N, Wismans JS. Estimation of spinal loading in vertical vibrations by numerical simulation. Clin Biomech (Bristol, Avon). 2003;18:800–11.
12. Fritz M. Description of the relation between the forces acting in the lumbar spine and whole-body vibrations by means of transfer functions. Clin Biomech (Bristol, Avon). 2000;15:234–40.
13. Thomas M, Lakis AA, Sassi S. Adverse health effects of long-term whole-body random vibration exposure. In: Recent research. Development in sound and vibration 2. Trivandrum, Kerala, India: Transworld Research Network; 2004. p. 55–73.
14. Lavaste F, Skalli W, Robin S, Roy-Camille R, Mazel C. Three-dimensional geometrical and mechanical modelling of the lumbar spine. J Biomech. 1992; 25(10):1153–64.
15. Griffin MJ. Handbook of human vibrations. London, UK: Academic Press; 1990.
16. Ayari H, Thomas M, Doré S. Development of an injury risk factor for drivers, Revue Internationale sur l'Ingénierie des Risques Industriels. 2008;1(2):120–38. Retrieved July 26, from: http://jiiri.etsmtl.ca/Article3_Ayari_J-IRI.pdf
17. Keller TS. Predicting the compressive mechanical behavior of bone. J Biomech. 1994;27(9):1159–68.
18. Berry JL, Moran JM, Berg WS, Steffee AD. A morphometric study of human lumbar and selected thoracic vertebrae. Spine (Phila Pa 1976). 1987; 12(4):362–7.
19. Ayari H, Thomas M, Doré S, Serrus O. Evaluation of lumbar vertebra injury risk to the seated human body when exposed to vertical vibration. J Sound Vib. 2009;321(1–2):454–70 (DOI:10.1016/j.jsv.2008.09.046).
20. Izambert O, Mitton D, Thourot M, Lavaste F. Dynamic stiffness and damping of human intervertebral disc using axial oscillatory displacement under a free mass system. Eur Spine J. 2003;12(6):562–6.
21. Kasra M, Shirazi-Adl A, Drouin G. Dynamics of human lumbar intervertebral joints. Experimental and finite-element investigations. (Phila Pa 1976). 1992;17(1): 93–102.
22. International Organization for Standardization (ISO). Mechanical vibration and shock— evaluation of human exposure to whole-body vibration—part 5: Method for evaluation of vibration containing multiple shocks (Standard No. ISO 2631-5:2004). Geneva, Switzerland: ISO; 2004.
23. International Organization for Standardization (ISO). Mechanical vibration and shock—evaluation of human exposure to whole-body vibration—part 1: general requirements (Standard No. ISO 2631-1: 1997). Geneva, Switzerland: ISO; 1997.
24. McCalden RW, McGeough JA, Court-Brown CM. Age-related changes in the compressive strength of cancellous bone: the relative importance of changes in density and trabecular architecture. J Bone Joint Surg Am. 1997;79(3):421–7.
25. Ferguson SJ, Steffen T. Biomechanics of the aging spine. Eur Spine J. 2003; 12(Suppl. 2):S97–103.
26. Ettinger MP. Aging bone and osteoporosis: strategies for preventing fractures in the elderly. Arch Intern Med. 2003: 163(18):2237–46.
27. Adams M, Bogduk N, Burton K, Dolan P. Biomechanics of back pain. 2nd ed. Edinburgh, UK: Churchill Livingstone; 2006.
28. Hinz B, Blüthner R, Menzel G, Seidel H. Estimation of disc compression during transient whole-body vibration. Clin Biomech (Bristol, Avon). 1994;9(4):263–71 (DOI:http://dx.doi.org/10.1016/0268-0033(94)90009-4).